BIOCHEMISTRY
including biophysical chemistry & molecular biology

Article

pubs.acs.org/biochemistry

Drosophila Myosin-XX Functions as an Actin-Binding Protein To Facilitate the Interaction between Zyx102 and Actin

Yang Cao,[†,‡] Howard D. White,[§] and Xiang-dong Li*[,†,‡]

[†]Group of Cell Motility and Muscle Contraction, National Laboratory of Integrated Management of Insect Pests and Rodents, Institute of Zoology, Chinese Academy of Sciences, Beijing 100101, China

[‡]University of Chinese Academy of Sciences, Beijing 100049, China

[§]Department of Physiological Sciences, Eastern Virginia Medical School, Norfolk, Virginia 23507, United States

Supporting Information

ABSTRACT: The class XX myosin is a member of the diverse myosin superfamily and exists in insects and several lower invertebrates. DmMyo20, the class XX myosin in *Drosophila*, is encoded by *dachs*, which functions as a crucial downstream component of the Fat signaling pathway, influencing growth, affinity, and gene expression during development. Sequence analysis shows that DmMyo20 contains a unique N-terminal extension, the motor domain, followed by one IQ motif, and a C-terminal tail. To investigate the biochemical properties of DmMyo20, we expressed several DmMyo20 truncated constructs containing the motor domain in the baculovirus/Sf9 system. We found that the motor domain of DmMyo20 had neither ATPase activity nor the ability to bind to ATP, suggesting that DmMyo20 does not function as a molecular motor. We found that the motor domain of DmMyo20 could specifically bind to actin filaments in an ATP-independent manner and enhance the interaction between actin filaments and Zyx102, a downstream component of DmMyo20 in the Fat signaling pathway. These results suggest that DmMyo20 functions as a scaffold protein, but not as a molecular motor, in a signaling pathway controlling cell differentiation.

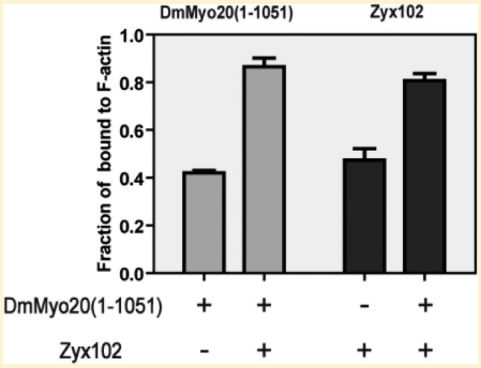

The myosin superfamily is currently comprised of more than 35 classes based on the motor domain sequence.[1] Myosins are involved in a variety of biological processes, such as muscle contraction, organelle transport, and cell polarization.[2−4] It is generally believed that myosin functions as a molecular motor that converts the energy from ATP hydrolysis into mechanical movement along actin filaments.

In spite of the high degree of homology, myosin motor domains have quite different motor properties. For example, myosin-5a and myosin-6 are high-duty motors that spend the majority of time attached to actin during the ATP hydrolysis cycle; by contrast, forms of myosin-2, such as skeletal muscle and smooth muscle myosin, are low-duty motors that spend most of time detached from actin. The high duty ratio allows one molecule or a few molecules of myosin-5a or myosin-6 to transport organelles along actin filaments, whereas a low duty ratio ensures that ensembles of muscle myosin molecules work efficiently without interfering with each other. The efficiencies of different myosin motors are quite variable, too. Fast myosin, such as plant myosin-11 (Chara myosin), has very high actin-activated ATPase activity (~400 head^{-1} s^{-1}) and sliding velocity (~50 μm s^{-1}),[5] whereas slow myosin, such as myosin-9b, has very low actin-activated ATPase activity (~0.2 head^{-1} s^{-1}) and gliding velocity (~0.02 μm s^{-1}).[6−9] Recently, it was reported that myosin-18 in *Drosophila melanogaster* displayed neither actin-activated ATPase activity nor ATP binding capacity.[10] These findings challenge the traditional concept that myosin always functions as a molecular motor.

Class XX myosin was first identified in the *Drosophila* genome and considered as an insect-specific myosin.[1,11,12] Blast of GenBank showed that class XX myosin also is present in several invertebrate species such as sea urchin, actinia, oysters, and Placozoa. Class XX myosin in *D. melanogaster*, DmMyo20, is encoded by *dachs*, which was first described by Bridges and Morgan.[14] Because DmMyo20 is located in the 2L position (29D1) of the *Drosophila* chromosome, DmMyo20 is also named Myo29D.[13,14] For the sake of clarity, we use DmMyo20 instead of Myo29D throughout this paper. Genetic studies showed that DmMyo20 acted as a downstream component of the Fat signaling pathway necessary for normal wing and leg appendage development.[11,15] Fat is an atypical cadherin located on the membrane function as a transmembrane receptor for the development signaling pathway. DmMyo20 interacts with proto-cadherins dachsous and is localized on the plasma membrane.[16,17] This membrane localization is inhibited by Fat.[11] DmMyo20 has downstream influences emanating from both the anterior−posterior (A−P) and dorsal−ventral (D−V) compartment boundaries.[18] When DmMyo20 accumulates at

Received: September 6, 2013
Revised: January 6, 2014
Published: January 6, 2014

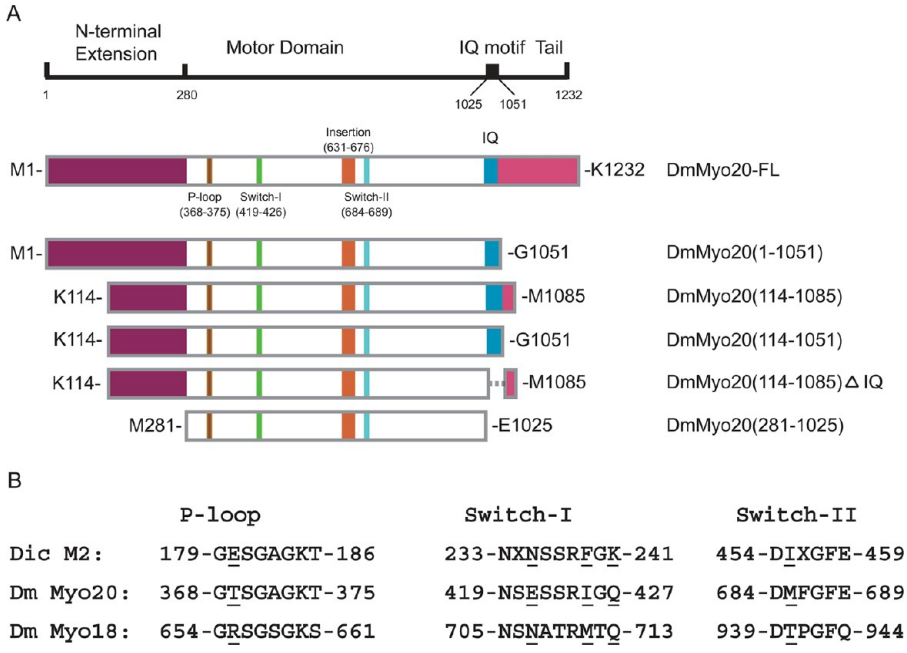

Figure 1. Schematics of DmMyo20 constructs. (A) Schematics of DmMyo20 constructs expressed in this study. (B) Sequence analysis of the P-loop, switch-I, and switch-II of *Dictyostelium* myosin-2 (Dic M2), DmMyo20, and *Drosophila* myosin-18 (Dm M18).

the membrane, it influences Warts (Wts) activity through Zyx102,[19] a *Drosophila* homologue of the vertebrate Zyxin, belonging to the LIM protein family. Most characterized LIM proteins are cytoskeleton-associated proteins that can interact directly or indirectly with F-actin.[20] It was proposed that DmMyo20 induces Zyx102 to expose its LIM domains to bind to Wts, thus promoting the degradation and inactivation of Wts.[19]

Sequence analysis shows that DmMyo20 has a specific N-terminal extension (amino acids 1−280), which is distinctive in the myosin families. According to the Simple Modular Architecture Research Tool (SMART), we found a short coiled-coil region (amino acids 20−49) and several low-complexity regions in the N-terminal extension. Sequence alignment revealed a highly conserved region (amino acids 137−152) in the N-terminal extension, suggesting a key role for this region in DmMyo20 functions. After the N-terminal extension is the motor domain (amino acids 281−1025) containing the putative ATP- and actin-binding sites. The motor domain is followed by a neck that contains only one IQ motif (amino acids 1026−1051) with the consensus sequence IQXXXRGXXXR, which might act as the binding sites for calmodulin (CaM) or CaM-like light chains. The 180 C-terminal amino acid residues form the tail domain (amino acids 1052−1232). According to the SMART, the tail domain contains some low-compositional complexity regions. Sequence alignment of the class XX myosins indicated that the C-terminal tail domain is highly conserved, which indicated that the class XX myosins might bind to other proteins to localize on the plasma membrane with this conserved domain.[16,21]

In this study, we found that DmMyo20 has no detectable ATPase activity and does not bind to ATP. Furthermore, we found DmMyo20 binds to F-actin in an ATP-independent manner and enhances the interaction between F-actin and Zyx102, a downstream target of DmMyo20. These results suggest that DmMyo20 does not function as a molecular motor but instead may function as a scaffold protein in the signaling pathway controlling cell differentiation.

EXPERIMENTAL PROCEDURES

Materials. Restriction enzymes and DNA-modifying enzymes were purchased from New England BioLabs (Beverly, MA), unless indicated otherwise. Actin was prepared from rabbit skeletal muscle acetone powder according to Spudich and Watt.[22] The anti-Flag M2 antibody, the anti-Flag M2 affinity gel, phosphoenolpyruvate, 2,4-dinitrophenylhydrazine, and pyruvate kinase were from Sigma Co. (St. Louis, MO). The Flag peptide (DYKDDDDK) was synthesized by Augct Co. (Beijing, China). Phenyl Sepharose 6 Fast Flow was from GE Healthcare. Oligonucleotides were synthesized by Invitrogen Co. The anti-HA mouse antibody was from Medical & Biological Laboratories Co., Ltd. The HRP-conjugated goat anti-mouse antibody was from Abmart Co. (Shanghai, China). [α-^{32}P]ATP (~5000 Ci/mmol, 10 mCi/ml) was from Fu Rui Bioengineer Co. (Beijing, China).

Cloning and Expression of DmMyo20 Constructs. All DmMyo20 constructs (Figure 1A) in this study were created from pUAST-d (DmMyo20-FL/pUAST) (provided by K. D. Irvine, Rutgers, the State University of New Jersey, Piscataway, NJ).[11] DmMyo20 cDNA was subcloned into modified baculovirus transfer vector pFastHFTc,[23] and recombinant baculoviruses were prepared using the Bac-To-Bac system (Invitrogen). Sf9 cells were co-infected with the recombinant viruses of DmMyo20 heavy chain and DmCaM. The expressed DmMyo20 protein contained an N-terminal His tag and Flag tag (MSYYH HHHHH DYKDD DDKNI PTTEN LYFQG AMGIR NSKAY VDELT SPA). The expressed DmMyo20 proteins were purified by anti-Flag M2 affinity chromatography as described previously.[23,24] The purified DmMyo20 was dialyzed against 5 mM Tris-HCl (pH 7.5), 200 mM NaCl, 5 mM EGTA (pH 8.0), 1 mM DTT, and 10% glycerol before being aliquoted and stored at −80 °C.

dx.doi.org/10.1021/bi401236c | *Biochemistry* 2014, 53, 350−360

Approximately 0.8 mg of DmMyo20 truncated constructs except DmMyo20(1−1051) was obtained from 0.3 L of Sf9 cell cultures, and approximately 0.3 mg of DmMyo20(1−1051) was obtained from 0.5 L of Sf9 cell cultures. The concentrations of the purified DmMyo20 constructs except DmMyo20(1−1051) were estimated by the absorbance at 280 nm, using the following molar extinction coefficients: 65380 L mol^{-1} cm^{-1} for DmMyo20(114−1085), 65380 L mol^{-1} cm^{-1} for DmMyo20(114−1051), 41340 L mol^{-1} cm^{-1} for DmMyo20(114−1085)ΔIQ, and 41220 L mol^{-1} cm^{-1} for DmMyo20(281−1025). These molar extinction coefficients were calculated on the basis of the amino acid composition of DmMyo20 heavy chain and bound DmCaM. Because the concentration of purified DmMyo20(1−1051) was too low to be accurately measured on the basis of the absorbance at 280 nm, its concentration was estimated by sodium dodecyl sulfate−polyacrylamide gel electrophoresis (SDS−PAGE) and Coomassie blue staining with smooth muscle myosin as a standard.

Cloning and Expression of DmCaM and Zyx102. Reverse transcripts of the cDNA of DmCaM (*Drosophila* calmodulin, GenBank entry CG8472) were obtained from total larval RNA using AccuScript Reverse Transcriptase (Stratagene) and amplified by polymerase chain reaction (PCR) with primers 5′-ATACATATGGCCGATCAGCTGACAG-3′ (NdeI site underlined) and 5′-ATCGGATCCATAGCAACAGCGTG-3′ (BamHI site underlined) and inserted into the NdeI and BamHI sites of the pT7 vector. To express DmCaM in *Escherichia coli*, BL21(DE3) was transformed with DmCaM into a pT7 expression vector and then cultured in 500 mL of LB medium supplemented with 50 μg/mL ampicillin at 37 °C until the OD_{600} reached 0.8−1.0. After being induced with 0.2 mM isopropyl 1-thio-β-D-galactopyranoside (IPTG), the cells were cultured overnight at 16 °C. The expressed DmCaM was purified using Phenyl-Sepharose as described for human CaM.[25] Approximately 30 mg of DmCaM was obtained from 0.5 L of an *E. coli* cell cultures. The DmCaM concentration was determined by the absorbance at 280 nm, using a molar extinction coefficient of 1280 L mol^{-1} cm^{-1}.

To prepare a recombinant baculovirus encoding DmCaM, the cDNA of DmCaM was amplified with primers 5′-ATAGGATCCGCCGATCAGCTGACAG-3′ (BamHI site underlined) and 5′-ATCCTCGAGATAGCAACAGCGTG-3′ (XhoI site underlined) and subcloned into the BamHI and XhoI sites of pFastBac1. The cDNA of *D. melanogaster* Zyx102 (GenBank entry CG32018) was reverse transcribed from larval total RNA, amplified by PCR with primers 5′-ACTGGCGGCCGCATGGAGTCTGTGGCCCAGCAAC-3′ (underlined, NotI site) and 5′-TCAGCTCGAGGACGTCAGAACATTAAATTGAG-3′ (underlined, XhoI site), and subcloned into the NotI and XhoI sites of pFastHHATc, a modified pFastBacHTc containing an N-terminal His tag and an HA tag (YPYDVPDYA) or pFastHFTc.[23] Recombinant baculoviruses were prepared using the Bac-To-Bac system (Invitrogen).

To express Zyx102 with a His tag and an HA tag, Sf9 cells were infected by a recombinant baculovirus encoding Zyx102 and cultured for 60 h. The expressed Zyx102 was purified by Ni^{2+}-NTA agarose affinity chromatography as described previously,[26] except that the purified Zyx102 was dialyzed against 5 mM Tris-HCl (pH 7.5), 200 mM NaCl, 5 mM EGTA (pH 8.0), 1 mM DTT, and 10% glycerol before being aliquoted and stored at −80 °C. Zyx102 with an N-terminal Flag tag was expressed in Sf9 cells and purified by anti-Flag M2 affinity chromatography as described above.[23,24] Approximately 0.3 mg of Zyx102 was obtained from 0.5 L of Sf9 cell cultures. The Zyx102 concentration was estimated by SDS−PAGE and Coomassie blue staining with smooth muscle myosin as a standard.

Preparation of Other Proteins. Smooth muscle heavy meromyosin (SmM-HMM or Sm-1063), smooth muscle myosin subfragment 1 (SmM-S1 or Sm-849), and myosin-5a-S1 (a truncated myosin-5a-containing motor domain and first IQ motif, M5a-791) was expressed in Sf9 cells and purified by anti-Flag M2 affinity chromatography as described previously.[25,27] Skeletal muscle myosin was prepared from rabbit muscle according to a published method.[28]

CaM Gel Shift Assays. CaM displays a unique electrophoretic mobility shift during SDS−PAGE in response to Ca^{2+}.[29] To determine whether the light chain of DmMyo20 is CaM, the purified DmMyo20 constructs, DmCaM (CaM of *D. melanogaster*), or vertebrate CaM was incubated with 5 mM EGTA or 5 mM $CaCl_2$ at room temperature for 5 min, mixed with SDS loading buffer, and boiled for 5 min, before being separated by SDS−PAGE (4 to 20%) and visualized by Coomassie blue staining.

Circular Dichroism (CD) and Thermostability of Myosins. Before CD analysis, myosin samples were dialyzed against 50 mM Tris-HCl (pH 7.5), 0.2 M NaCl, 5 mM EGTA (pH 8.0), 1 mM DTT, and 10% glycerol and clarified by centrifugation at 100000*g* for 10 min (Beckman Optima MAX-XP) at 4 °C. CD spectra of myosin (3 μM) were recorded with Chirascan-plus CD spectrometer using wavelengths from 200 to 280 nm with 1 nm increments per 2.5 s. At least three scans were taken. The thermostability of myosin was recorded using CD signaling at 222 nm with temperatures increasing from 20 to 90 °C. The baseline of the solution was excluded from the statistical results.

ATPase Assay. The Mg^{2+}-ATPase activity of DmMyo20 was measured in a plate-based ATP assay system as described previously.[25] The Mg^{2+}-ATPase activities of DmMyo20 were measured in a solution containing 20 mM MOPS (pH 7.0), 60 mM NaCl, 1 mM $MgCl_2$, 1 mM DTT, 0.25 mg/mL BSA, 12 μM CaM, 0.5 mM ATP, 2.5 mM PEP, 20 units/mL pyruvate kinase, 1 mM EGTA, ∼2 μM DmMyo20, and 0 or 50 μM actin at 25 °C for up to 6 h. The ATPase activity of myosin-5a-S1 was measured similarly except that 20−50 nM myosin-5a-S1 was used with an incubation time of up to 1 h.

The Ca^{2+}-ATPase activity and K^+(EDTA)-ATPase activity were measured as described previously[30] with minor modifications. The Ca^{2+}-ATPase activity of DmMyo20 was measured in a solution containing 0.5 M KCl, 30 mM Tris-HCl (pH 8.5), 10 mM $CaCl_2$, 0.5 mM ATP, 0.25 mg/mL BSA, and ∼2 μM DmMyo20(114−1051) at 25 °C for up to 8 h. The Ca^{2+}-ATPase activity of SmM-S1 or SmM-HMM was measured similarly except that 60−80 nM myosins were used and the incubation time was ≤20 min. The amount of liberated phosphate was determined by the malachite green method.[31] The K^+(EDTA)-ATPase activity was measured similarly except that 10 mM $CaCl_2$ was substituted with 10 mM EDTA.

Photoaffinity Labeling of Myosin with ATP. Photoaffinity labeling was performed as described previously.[30,32] DmMyo20(114−1051) or SmM-HMM was tested for binding of ATP by UV cross-linking to [α-^{32}P]ATP. The reaction mixture contained 1 μM myosin head, 3 or 30 μM [α-^{32}P]ATP (specific activity of 2381 or 233 Ci/mmol), 30 mM Tris-HCl (pH 7.5), 1 mM $MgCl_2$, and 1 mM EGTA. Cross-linking was

conducted on ice at a distance of approximately 4 cm for 15 min with an ultraviolet light (18 W) at 254 nm. The protein was precipitated via the addition of cold 5% trichloroacetic acid and collected by centrifugation. The pellets were washed once with the same solution, dissolved in 15 μL of SDS loading buffer, and then subjected to SDS−PAGE and autoradiography using a storage phosphor screen (Amersham Biosciences Typhoon 9400 variable mode imager).

Excitation and Emission Spectra of Deac-Amino Nucleotides. The emission and excitation spectra of nucleotide analogue 3′-(7-diethylaminocoumarin-3-carbonylamino)-3′-deoxy-ATP (Deac-amino-ATP) in the presence and absence of DmMyo20 constructs (1 μM) or smooth muscle heavy meromyosin (SmM-HMM) were recorded as described previously.[33] The binding reaction mixtures contained 0.1 μM myosin head, 0.05 μM Deac-amino-ATP, 10 mM MOPS (pH 7.0), 25 mM KCl, 3 mM $MgCl_2$, 1 mM EGTA, and 1 mM DTT at 20 °C. All proteins were clarified by centrifugation at 100000*g* for 10 min (Beckman Optima MAX-XP) at 4 °C just prior to the analysis. Excitation spectra were recorded using an emission wavelength of 470 nm, and emission spectra were recorded using an excitation wavelength of 430 nm. The emission and excitation spectra were recorded in a Hitachi F-4500 FL spectrophotometer with a thermostatic cell house at 20 °C.

Co-Immunoprecipitation of Zyx102 and DmMyo20. Co-immunoprecipitation of HA-tagged Zyx102 and Flag-tagged DmMyo20(1−1051) or DmMyo20(114−1051) was performed as described previously.[26] Briefly, 0.7 μM DmMyo20(1−1051) or DmMyo20(114−1051) was incubated with 2.8 μM Zyx102 in solution A [50 mM Tris-HCl (pH 7.5), 150 mM NaCl, 2 mM EGTA, and 1 mM DTT] at 4 °C for 30 min. The reaction mixture was mixed with 10 μL of anti-Flag M2 agarose, incubated at 4 °C for 2 h, spun down, and washed six times with 200 μL of solution A. The bound proteins were eluted with 25 μL of 0.3 mM Flag peptide in solution A, analyzed by SDS−PAGE (4 to 20%), and visualized by Coomassie blue staining or Western blot using the HRP-conjugated anti-Flag M2 antibody (for Flag-tagged DmMyo20 constructs) or the anti-HA antibody (for HA-tagged Zyx102).

Actin Cosedimentation Assay. DmMyo20 (0.6−2.1 μM) was incubated with rabbit skeletal actin (0−50 μM) in a 50 μL solution of 20 mM Tris-HCl (pH 7.5), 200 mM NaCl, 5 mM EGTA, 2 mM $MgCl_2$, and 1 mM DTT at 4 °C for 1 h. ATP or ADP was added to the reaction mixture before centrifugation. The mixtures were centrifuged at 80000 rpm (Beckman Optima MAX-XP, TLA-120.1 rotor) for 15 min at 4 °C. Equal portions of the pellet and the supernatant were subjected to SDS−PAGE and Coomassie blue staining. The amounts of DmMyo20 and Zyx102 were quantified using NIH ImageJ version 1.42Q.

Actin Gliding Assay. DmMyo20 (300 nM) or skeletal muscle myosin (20 nM) in buffer B [25 mM HEPES (pH 7.5), 25 mM KCl, 6 mM $MgCl_2$, 1 mM EGTA, 2000 units/mL catalase, 40 units/mL glucose oxidase, 3.0 mg/mL glucose, and 140 mM β-mercaptoethanol] was absorbed onto a nitrocellulose-coated coverslip at 4 °C for 10 min. The coverslip was washed with BSA [0.5 mg/mL, 25 μL, in 25 mM HEPES (pH 7.4), 25 mM KCl, 6 mM $MgCl_2$, and 14 mM β-mercaptoethanol] to remove the unbound proteins and block the surface. Rhodamine phalloidin-labeled F-actin [0.5 μM, 25 μL, in 20 mM imidazole (pH 7.5), 25 mM KCl, 5 mM $MgCl_2$, and 0.02% NaN_3] was applied to the coverslip and incubated at 4 °C for 5 min. The coverslip was washed three times with 25 μL of buffer A with or without 2 mM ATP to remove the unbound F-actin. The bound F-actin was visualized under an Olympus IX71 inverted fluorescent microscope.

RESULTS

Identification of Calmodulin as the Light Chain of DmMyo20. DmMyo20 contains 1232 amino acid residues, including a unique N-terminal extension (amino acids 1−280), the motor domain (amino acids 281−1025), one IQ motif (amino acids 1026−1051), and a C-terminal tail domain (amino acids 1052−1232).[11] We analyzed the N-terminal extension using SMART (the Simple Modular Architecture Research Tool) but did not identify any structural motifs except a short coiled-coil region (amino acids 20−49). Sequence alignment of the class XX myosins showed a highly conserved region (amino acids 137−152) in the N-terminal extension. The highly conserved sequences might play a key role in the protein function. To investigate the structure and function of DmMyo20, we created a number of DmMyo20 truncated constructs containing the intact or truncated N-terminal extension, the motor domain, and the IQ motif (Figure 1A). DmMyo20 truncated constructs were expressed in the baculovirus/Sf9 expression system and purified by anti-Flag affinity chromatography (Figure 2B).

DmMyo20 contains one IQ motif (amino acids 1026−1051) with the consensus sequence IQXXXRGXXXR, which might act as the binding sites for CaM or CaM-like light chains. To identify the light chain associated with DmMyo20, we infected Sf9 cells with a recombinant baculovirus encoding DmMyo20(114−1051) containing part of the N-terminal extension, the motor domain, and the putative IQ motif. The expressed protein was purified by anti-Flag M2 affinity chromatography. We noticed a band of ∼17 kDa that copurified with DmMyo20(114−1051) during SDS−PAGE (Figure 2A, lanes 5 and 6). We suspected that the ∼17 kDa band was Sf9 endogenous CaM and therefore performed the gel shift assay. It was known that CaM displays a unique electrophoretic mobility shift during SDS−PAGE in response to Ca^{2+}.[29] As expected, the ∼17 kDa band displayed a mobility shift in response to Ca^{2+} during SDS−PAGE similar to that of vertebrate CaM and DmCaM (*Drosophila* calmodulin) (Figure 2A), indicating that the ∼17 kDa band was CaM. Because Sf9 endogenous CaM might not be sufficient to saturate the binding site in DmMyo20, we coexpressed DmMyo20(114−1051) with DmCaM in Sf9 cells. Purified DmMyo20(114−1051) contained DmCaM with a stoichiometry of 0.72 (DmCaM to heavy chain) (Figure 2B, lane 2).

To determine if the putative IQ motif is the binding site of DmCaM, we coexpressed DmCaM with DmMyo20(114−1085) or DmMyo20(114−1085)ΔIQ, which does not contain the predicted IQ motif (amino acids 1026−1051) (Figure 1A). We found that a stoichiometric amount of DmCaM was associated with DmMyo20(114−1085), but not with DmMyo20(114−1085)ΔIQ (Figure 2B, lane 1 vs lane 3), indicating that the putative IQ motif in the fragment of amino acids 1026−1051 is the only DmCaM-binding site. Consistently, we did not detect the association of DmCaM with DmMyo20(281−1025) (Figure 2B, lane 4). These results indicate that DmMyo20 has only one IQ motif, which is associated with DmCaM.

Circular Dichroism (CD) Spectrum and Thermostability of DmMyo20. To examine the proper folding of

dx.doi.org/10.1021/bi401236c | *Biochemistry* 2014, 53, 350−360

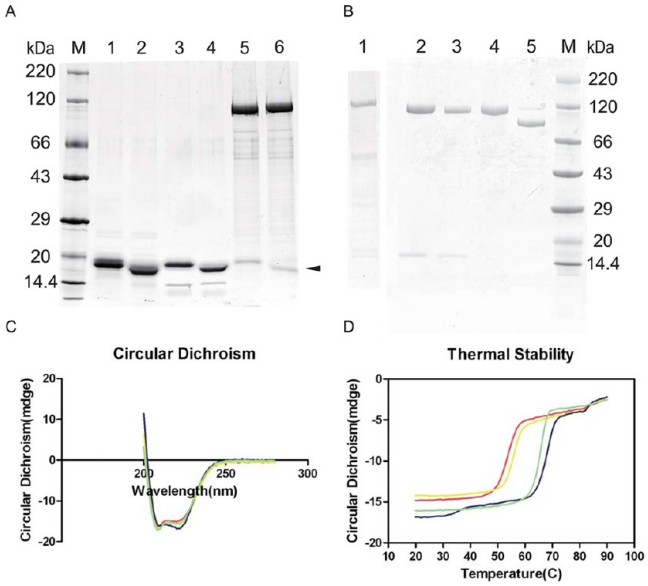

Figure 2. Identification of the light chain of DmMyo20 and the structural property of DmMyo20. (A) Identification of calmodulin as the light chain of DmMyo20. Purified CaM and DmMyo20(114−1051) were analyzed by SDS−PAGE (4 to 20%): lanes 1 and 2, mammalian CaM; lanes 3 and 4, *Drosophila* CaM (DmCaM); lanes 5 and 6, purified DmMyo20(114−1051) that was expressed in Sf9 cells without extra CaM. Lanes 1, 3, and 5 were run under EGTA conditions, whereas lanes 2, 4, and 6 were run under Ca^{2+} conditions. For details, see Experimental Procedures. (B) SDS−PAGE (4 to 20%) of the purified DmMyo20 constructs: lane 1, DmMyo20(1−1051); lane 2, DmMyo20(114−1085); lane 3, DmMyo20(114−1051); lane 4, DmMyo20(114−1085)ΔIQ; lane 5, DmMyo20(281−1025). Lane M contained the molecular mass markers with the molecular masses indicated at the right. (C) CD spectra of DmMyo20(114−1051) (red), DmMyo20(114−1085) (yellow), myosin-5a-S1 (blue), and SmM-S1 (green) (3 μM each) recorded at 25 °C. (D) Thermostability of DmMyo20, SmM-S1, and myosin-5a-S1. CD signaling of myosin at 222 nm was recorded from 20 to 90 °C for DmMyo20(114−1051) (red), DmMyo20(114−1085) (yellow), SmM-S1 (green), and myosin-5a-S1 (blue).

DmMyo20, we compared the CD spectrum of DmMyo20(114−1051) and DmMyo20(114−1085) with those of myosin-5a-S1 and SmM-S1. Myosin-5a-S1 is a mouse myosin-5a truncated construct containing the motor domain and the first IQ motif with bound CaM,[25] and SmM-S1 is a chicken smooth muscle myosin truncated construct containing the motor domain and two IQ motifs with bound essential light chain and regulatory light chain.[27] We found that the CD spectra of DmMyo20(114−1051) and DmMyo20(114−1085) were similar to those of SmM-S1 and myosin-5a-S1 (Figure 2C), indicating that the DmMyo20 truncated constructs contained similar secondary structure and are likely to be properly folded.

The loss of CD signals with an increase of temperature can be used to quantify the thermostability of a protein. Therefore, we measured the CD signaling (at 222 nm) of DmMyo20 from 20 to 90 °C. We found that the level of CD signaling of DmMyo20(114−1051) and DmMyo20(114−1085) decreased with an increase in temperature, and the transition temperature was between 50 and 60 °C (Figure 2D). As controls, myosin-5a-S1 and SmM-S1 displayed similar thermostability except that the transition temperature was between 60 and 70 °C, ∼10 °C higher than that of DmMyo20. The relatively low thermostability of DmMyo20 probably reflects the fact that DmMyo20 is a protein from a cold-blooded animal (*Drosophila*), whereas myosin-5a-S1 and SmM-S1 are proteins from warm-blooded animals (mouse and chicken).

DmMyo20 Has neither ATPase Activity nor ATP Binding Ability. One basic property of myosin is the ability to hydrolyze ATP. So far, almost all characterized myosins, except a few such as *Limulus* myosin-3,[34] *Drosophila* myosin-18,[10] and mammalian myosin-18A,[35,36] have ATPase activity, which is enhanced by actin. The motor domain of DmMyo20 is 59 and 54% homologous with muscle myosin II and V of *D. melanogaster*, respectively.[13] The highly conserved sequences for ATP binding in the motor domain of myosin are largely preserved in DmMyo20, including the P-loop, switch-I, and switch-II (Figure 1B).

To determine whether DmMyo20 has ATPase activity, we measured the Mg^{2+}-ATPase activity of DmMyo20(114−1051) containing part of the N-terminal extension, the motor domain, and the IQ motif. The Mg^{2+}-ATPase activity of DmMyo20(114−1051) in the absence or presence of 50 μM actin was below the detection limit of our ATPase assay system (∼0.002 s^{-1} $head^{-1}$) (Table 1). Similar results were found for other DmMyo20 constructs, including DmMyo20(114−1085) and DmMyo20(281−1025). In contrast, myosin-5a-S1, a truncated myosin-5a containing the motor domain and the first IQ motif, showed substantial ATPase activity in the absence of actin (0.027 ± 0.001 s^{-1} $head^{-1}$), which was enhanced ∼200-fold by 50 μM actin (11.015 ± 0.027 s^{-1} $head^{-1}$). Therefore, the actin-activated ATPase activity of DmMyo20 constructs, if is exists, is at least 5000 times lower than that of myosin-5a-S1.

Table 1. Mg^{2+}-ATPase Activities of Myosins (s^{-1} $head^{-1}$)

	Mg^{2+}-ATPase[a]	
myosin	basal activity	actin-activated
myosin-5a-S1	0.027 ± 0.001	11.015 ± 0.027
DmMyo20(114−1051)	<0.002	<0.002

[a] Mg^{2+}-ATPase activity of myosin was measured in 20 mM MOPS (pH 7.0), 60 mM NaCl, 1 mM $MgCl_2$, 1 mM DTT, 0.25 mg/mL BSA, 12 μM CaM, 0.5 mM ATP, 2.5 mM PEP, 20 units/mL pyruvate kinase, 1 mM EGTA, and ∼2 μM DmMyo20 or 20−50 nM myosin-5a-S1 in the absence (basal) or presence (actin-activated) of 50 μM actin. The background ATPase activity was removed. All the results are means ± the standard error (n = 3).

We also measured the ATPase activity of DmMyo20(114−1051) under nonphysiological conditions. Historically, Ca^{2+}-ATPase and K^+(EDTA)-ATPase have been used to characterize the enzymatic activity of muscle myosin ATPase. We could not detect significant ATPase activity of DmMyo20(114−1051) under either Ca^{2+}-ATPase or K^+(EDTA)-ATPase assay conditions. In contrast, SmM-HMM and SmM-S1 showed normal Ca^{2+}-ATPase and K^+(EDTA)-ATPase activity (Table 2).

To determine whether DmMyo20 was able to bind ATP, we took two approaches. First, we examined the fluorescence intensity of Deac-amino-ATP in the presence of DmMyo20. Deac-amino-ATP is a fluorescent ATP analogue and has been used in the field of myosin dynamics.[33,37] Unbound Deac-amino-ATP has a relatively low fluorescence intensity that is usually enhanced up to ∼20-fold upon binding to myosins.[33] We found that the fluorescence intensity of Deac-amino-ATP

dx.doi.org/10.1021/bi401236c | *Biochemistry* 2014, 53, 350−360

Table 2. Ca^{2+}-ATPase Activities and K^+(EDTA)-ATPase Activities of Myosins (s^{-1} $head^{-1}$)

myosin	Ca^{2+}-ATPase[a]	K^+(EDTA)-ATPase[a]
SmM-HMM	0.637 ± 0.001	1.506 ± 0.059
SmM-S1	0.579 ± 0.047	1.219 ± 0.047
DmMyo20(114−1051)	<0.002	<0.002

[a] Ca^{2+}-ATPase activity was measured in a buffer containing 0.5 M KCl, 30 mM Tris-HCl (pH 8.5), 10 mM $CaCl_2$, 0.5 mM ATP, and ~2 μM DmMyo20(114−1051), 60−80 nM SmM-S1 (smooth muscle myosin subfragment 1), or SmM-HMM. The K^+(EDTA)-ATPase activity was measured similarly except that 10 mM $CaCl_2$ was replaced with 10 mM EDTA. All the results are means ± the standard error (n = 3).

did not increase upon addition of DmMyo20(114−1051), whereas that of Deac-amino-ATP increased 15-fold upon addition of SmM-HMM (Figure 3).

Second, we detected ATP binding of DmMyo20(114−1051) using radioactive ATP. [α-^{32}P]ATP can be cross-linked with myosin upon UV irradiation and detected by autoradiography.[38] As shown in Figure 4, a significant amount of SmM-HMM cross-linked with ATP upon UV irradiation was clear and definite at 3 or 30 μM ATP. In contrast, there was no detectable cross-linking between ATP and DmMyo20(114−1051) even at the higher ATP concentration (30 μM). In summary, these results clearly indicate that that the DmMyo20 motor domain has no ATPase activity and cannot bind to ATP.

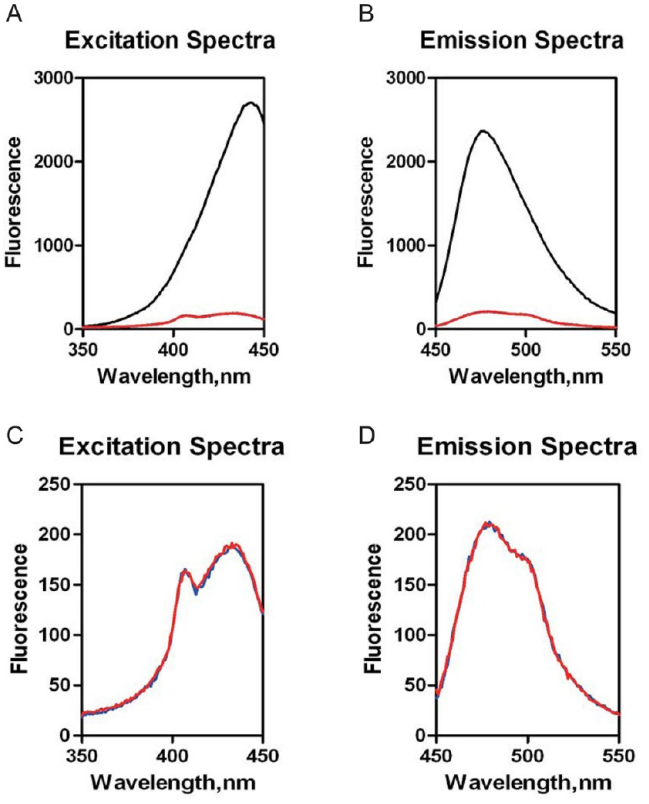

Figure 3. Excitation and emission spectra of Deac-amino nucleotides in the presence and absence of DmMyo20 or SmM-HMM. (A) Excitation and (B) emission spectra of Deac-amino-ATP in binding assays using expressed DmMyo20(114−1051) (red) in comparison to the fluorescence baseline of the Deac-amino moiety (blue) contrasted with smooth muscle heavy meromyosin (SmM-HMM) (black). Excitation (C) and emission (D) spectra of Deac-amino-ATP assays using only expressed DmMyo20(114−1051) (red) in comparison to the fluorescence baseline of the Deac-amino moiety (blue) shown on an expanded scale. Final concentrations in the assays were 0.1 μM DmMyo20(114−1051) or SmM-HMM and 0.05 μM Deac-amino-ATP in 0.5 M KCl, 10 mM MOPS (pH 7.0), 3 mM $MgCl_2$, 1 mM EGTA, and 1 mM DTT.

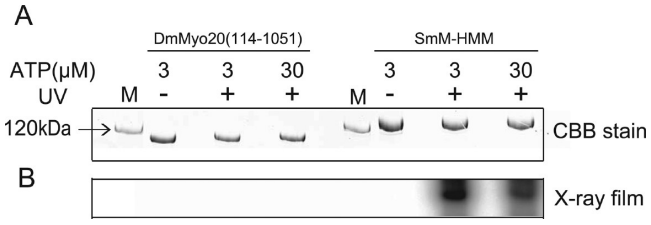

Figure 4. Photoaffinity labeling of DmMyo20 with radioactive ATP. Smooth muscle myosin heavy meromyosin (SmM-HMM) or DmMyo20(114−1051) (1 μM) was incubated with [α-^{32}P]ATP (3 or 30 μM) and subjected to UV irradiation, SDS−PAGE, and autoradiography: (A) Coomassie blue staining and (B) autoradiography.

DmMyo20 Binds with F-Actin in an ATP-Independent Manner. All characterized myosins thus far interact with F-actin, and most of these interactions are ATP-dependent. To assess the ability of DmMyo20 to bind to F-actin, we performed an actin cosedimentation assay. As shown in Figure 5A, a small amount of DmMyo20(114−1051) cosedimented with F-actin. The amount of actin that cosedimented with DmMyo20(114−1051) was not influenced by the addition of ATP or ADP, whereas SmM-HMM cosedimented with actin in an ATP-dependent manner (Figure 5A). Similar results were found for DmMyo20(281−1025) and DmMyo20(114−1085) (data not shown), indicating that DmMyo20 associates with actin through the motor domain. To assess the affinity of DmMyo20 for actin, we cosedimented DmMyo20(114−1051) with various concentrations of actin (from 0 to 50 μM) (Figure 5C). We found that <30% of DmMyo20(114−1051) was cosedimented with actin even at the maximal concentration of actin tested (50 μM) (Figure 5C). The dissociation constant (K_d) determined by fitting the binding curve to a hyperbolic equation was determined to be 37.0 ± 2.7 μM with saturation as 44.9 ± 3.4%. The experimental data shown in Figure 5B are representative of multiple attempts (n = 3; mean ± standard deviation).

We found that the DmMyo20 construct with the intact N-terminal extension, i.e., DmMyo20(1−1051), displayed stronger affinity for actin than the DmMyo20 construct with the truncated N-terminal extension, i.e., DmMyo20(114−1051) (Figure 5D). The estimated dissociation constant (K_d) of DmMyo20(1−1051) for actin was 7.4 ± 2.0 μM with saturation as 84.9 ± 4.9% (Figure 5B).

To further examine the interaction between DmMyo20 and F-actin, we took an approach similar to the actin gliding assay. DmMyo20(114−1051) was first absorbed onto a nitrocellulose-coated coverslip; then fluorescence-labeled F-actin was applied to the coverslip, and the bound fluorescence-labeled F-actin was visualized under a fluorescence microscope. We found that a substantial amount of fluorescence-labeled F-actin was retained by DmMyo20(114−1051), and the amount of retained F-actin was not affected by ATP (Figure 6B,E). In contrast, the retention of fluorescence-labeled F-actin by skeletal muscle myosin was ATP-dependent (Figure 6C,F). These results confirm the result of actin cosedimentation assay; i.e., the DmMyo20 motor domain binds to F-actin in an ATP-

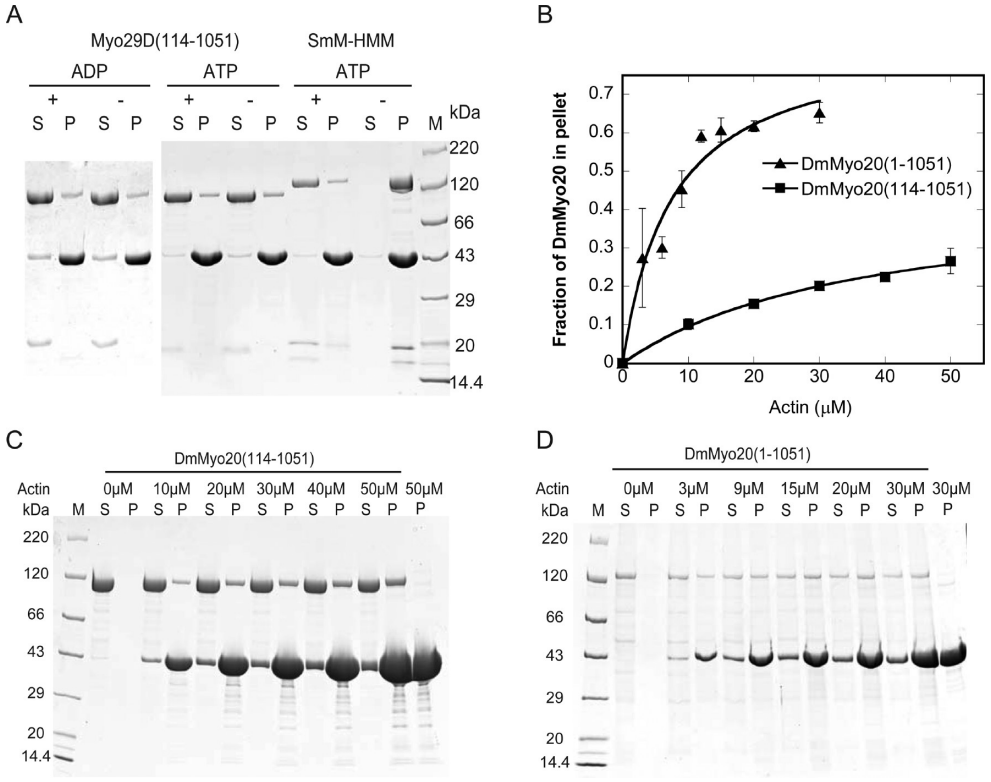

Figure 5. DmMyo20 cosedimented with actin in an ATP-independent manner. (A) DmMyo20(114−1051) or smooth muscle heavy meromyosin (SmM-HMM) was incubated with 10 μM actin in the absence or presence of ATP (ADP) and then subjected to ultracentrifugation. The supernatants (S) and the pellets (P) were analyzed by SDS−PAGE (4 to 20%) and visualized by Coomassie blue staining. (B) Fractions of DmMyo20 cosedimented were quantified by densitometry and plotted vs actin concentration. The dissociation constant (K_d) was determined by fitting the binding curve to the hyperbolic equation $B = B_{max}/(1 + K_d/[\text{actin}])$, where B represents the fraction of myosin that cosedimented with actin and K_d represents the dissociation constant. Data are the average of three independent assays. The estimated K_d and B_{max} of DmMyo20(114−1051) for actin were 37.0 ± 2.7 μM and 44.9 ± 3.4%, respectively. The estimated K_d and B_{max} of DmMyo20(1−1051) for actin were 7.4 ± 2.0 μM and 84.9 ± 4.9%, respectively. (C) DmMyo20(114−1051) was incubated with various concentrations of actin (0−50 μM) in the absence of ATP and then subjected to ultracentrifugation. Equal portions of supernatants and pellets were analyzed by SDS−PAGE and visualized by Coomassie blue staining. (D) DmMyo20(1−1051) was incubated with various concentrations of actin (0−30 μM) in the absence of ATP and then subjected to ultracentrifugation. Equal portions of supernatants and pellets were analyzed by SDS−PAGE and visualized by Coomassie blue staining.

independent manner. It is worth noting that we did not observe the movement of F-actin by DmMyo20(114−1051) in the presence of ATP.

DmMyo20 Enhances the Association between Zyx102 and F-Actin. The *Drosophila* Zyxin family gene, Zyx102, is a downstream component of DmMyo20 in the Fat signaling pathway. It was reported that Zyx102 and DmMyo20 can co-immunoprecipitate (Co-IP) from the lysate of S2 cells expressing these two proteins,[19,39] suggesting a direct or indirect interaction between Zyx102 and DmMyo20. Moreover, the ability of the DmMyo20 N-terminal extension to bind to Zyx102 was stronger than that of the motor domain. To determine whether the interaction between DmMyo20 and Zyx102 is direct or indirect, we performed Co-IP using purified DmMyo20 constructs and HA-tagged Zyx102. HA-tagged Zyx102 was first incubated with Flag-tagged DmMyo20(1−1051) or DmMyo20(114−1051) and then immunoprecipitated with anti-Flag affinity agarose and eluted with the Flag peptide. The eluted proteins were separated by SDS−PAGE and detected by an anti-Flag or anti-HA antibody (Figure 7A). Both DmMyo20(1−1051) and DmMyo20(114−1051) could Co-IP Zyx102, indicating a direct interaction between DmMyo20 and Zyx102. The amount of Zyx102 Co-IP by DmMyo20(1−1051) was ∼10 times more than that Co-IP by DmMyo20(114−1051) (Figure 7A), suggesting that the N-terminal extension of DmMyo20 plays a major role in binding with Zyx102. To quantify the interaction between DmMyo20(1−1051) and Zyx102, we performed Co-IP using 1.1 μM DmMyo20(1−1051) and 0−4 μM Zyx102 and visualized the eluted proteins with Coomassie blue staining (Figure S1 of the Supporting Information). The amount of Zyx102 Co-IP with DmMyo20(1−1051) was far below the stoichiometry.

Zyxin, the mammalian homologue of Zyx102, can bind to F-actin with a low affinity.[40] We inferred that Zyx102 might have a similar ability to bind to F-actin. To examine this possibility, we performed actin cosedimentation with Flag-tagged Zyx102. Indeed, ∼47.4% of Zyx102 cosedimented with 10 μM actin (Figure 7B,C).

Because there is direct interaction between DmMyo20 and Zyx102 and both of them can bind to F-actin, we expected synergistic interactions among DmMyo20, Zyx102, and actin. To test this possibility, we performed actin cosedimentation with DmMyo20(1−1051) and Flag-tagged Zyx102 (Figure 7B). DmMyo20(1−1051) enhanced the amount of cosedimented Zyx102 from 47.4 to 80.7%, and Zyx102 enhanced the amount of actin-cosedimented DmMyo20(1−1051) from 42.0 to 86.6% (Figure 7C). These results suggest that DmMyo20 and Zyx102 might form a complex that interacts synergistically with F-actin.

dx.doi.org/10.1021/bi401236c | *Biochemistry* 2014, 53, 350−360

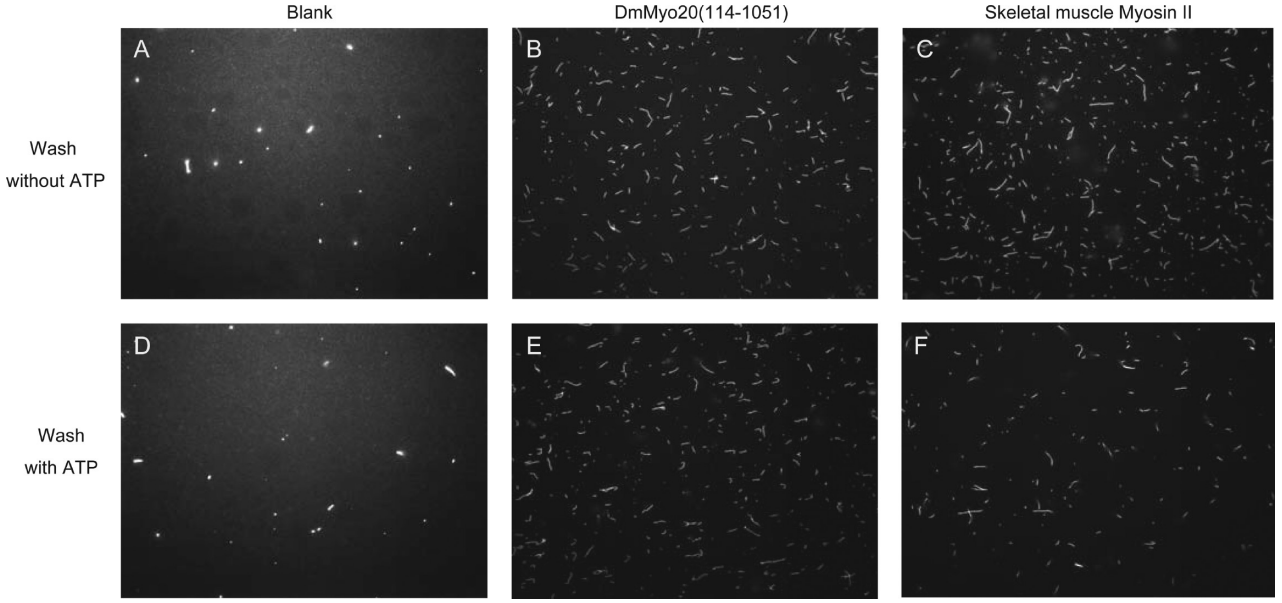

Figure 6. DmMyo20(114−1051) retained F-actin on a glass surface in an ATP-independent manner. DmMyo20(114−1051) (300 nM) or skeletal muscle myosin (20 nM) was absorbed onto a nitrocellulose-coated coverslip, and then the glass surface was blocked by BSA. Rhodamine phalloidin-labeled F-actin was perfused into the coverslip. After the unbound F-actin with or without ATP had been washed away, the remaining F-actin was visualized under a fluorescence microscope: (A and D) control without myosin, (B and E) DmMyo20(114−1051), and (C and F) skeletal muscle myosin II. (A−C) Washed without ATP and (D−F) washed with ATP.

In contrast to DmMyo20(1−1051), DmMyo20(114−1051) did not enhance the cosedimentation of Zyx102 with actin (Figure S2 of the Supporting Information), indicating that the N-terminal extension is essential for the synergistic interaction with actin.

DISCUSSION

Class XX myosin was first identified in the *Drosophila* genome and considered to be an insect-specific myosin.[1,11,12] Blast of GenBank showed that class XX myosin also is present in several invertebrate species such as sea urchin, actinia, oysters, and Placozoa. In this study, we found that DmMyo20, the class XX myosin in *D. melanogaster*, is a "motor incompetent" myosin, having neither ATPase activity nor ATP binding ability. Instead, it might function as an actin-binding protein and stimulate the binding of Zyx102 to F-actin.

The lack of ATPase activity and ATP binding ability of DmMyo20 could be attributed to several substitutions of the highly conserved sequences in the ATPase pocket of myosin, including the P-loop, switch-I, and switch-II (Figure 1B).

Compared to the P-loop of *Dictyostelium* myosin-2 (179-GESGAGKT-186, conserved residues underlined), that of DmMyo20 (368-G**T**SGAGKT-375) contains one E180T substitution. E180 is highly conserved residues among all types of myosin except a few unconventional myosins, including myosin-18. The crystal structure of the motor domain of *Dictyostelium* myosin-2 shows that E180 does not directly interact with the bound nucleotide; instead, E180 stabilizes the conformation of the P-loop by forming a hydrogen bond between its backbone carbonyl oxygen and the ε-amino group of K185 (K374 in DmMyo20),[41] suggesting the side chain of E180 is not essential for ATP binding. Indeed, we recently found that mutation of the E180-equivalent residue to threonine did not abolish the ATPase activity of smooth muscle myosin (our unpublished data). Thus, it is unlikely that the lack of ATPase activity in DmMyo20 is due to the absence of the conserved glutamic acid in P-loop.

A comparison of switch-I of *Dictyostelium* myosin-2 (233-NNNSSRFGK-241, conserved residues underlined) to that of DmMyo20 (419-NS**E**SSR**I**G**Q**-427) shows three substitutions of the conserved residues, i.e., N235E, F239I, and K241Q. The crystal structure of S1dC shows that N235, F239, and K241 are not directly involved in nucleotide binding but may play a role in maintaining the overall structure of the ATPase pocket.[41] The side chain of N235 is hydrogen-bonded to a water molecule, which in turn forms a hydrogen bond with the Mg^{2+} coordinating with the γ-phosphate moiety of ATP. However, neither N235 nor F239 seems to be essential for myosin ATPase and motor function, as both the N235A mutant and the F238A mutant of *Dictyostelium* myosin-2 retain nearly normal ATPase activity and *in vitro* actin gliding activity.[42] The ε-amino group of K241 (Q369 in DmMyo20) forms a salt bond with the carboxyl side chain of D454 in switch-II,[41] suggesting that K241 may play a role in maintaining the overall structure of the ATPase pocket.

Compared to switch-II of *Dictyostelium* myosin-2 (454-DISGFE-459, conserved residues underlined), that of DmMyo20 (684-D**M**FGFE-689) contains one substitution of the conserved residues, i.e., I455M. The side chain of I455 is in a hydrophobic pocket and undergoes a conformational change between the prehydrolysis and transition states.[43] However, the conserved I455 seems not to be essential for ATPase activity as mutations of the residue to alanine in *Dictyostelium* myosin-2 have no effect on the ATPase activity.[44]

The lack of ATPase activity and ATP binding ability of DmMyo20 could also be attributed to a unique insertion of 44 amino acid residues that precedes switch-II (Figure 1A). This 44-amino acid insertion that is not found in other myosins may potentially change the overall conformation of the ATPase pocket. Further experiments are needed to understand the role of this unique insertion in the function of DmMyo20.

dx.doi.org/10.1021/bi401236c | *Biochemistry* 2014, 53, 350−360

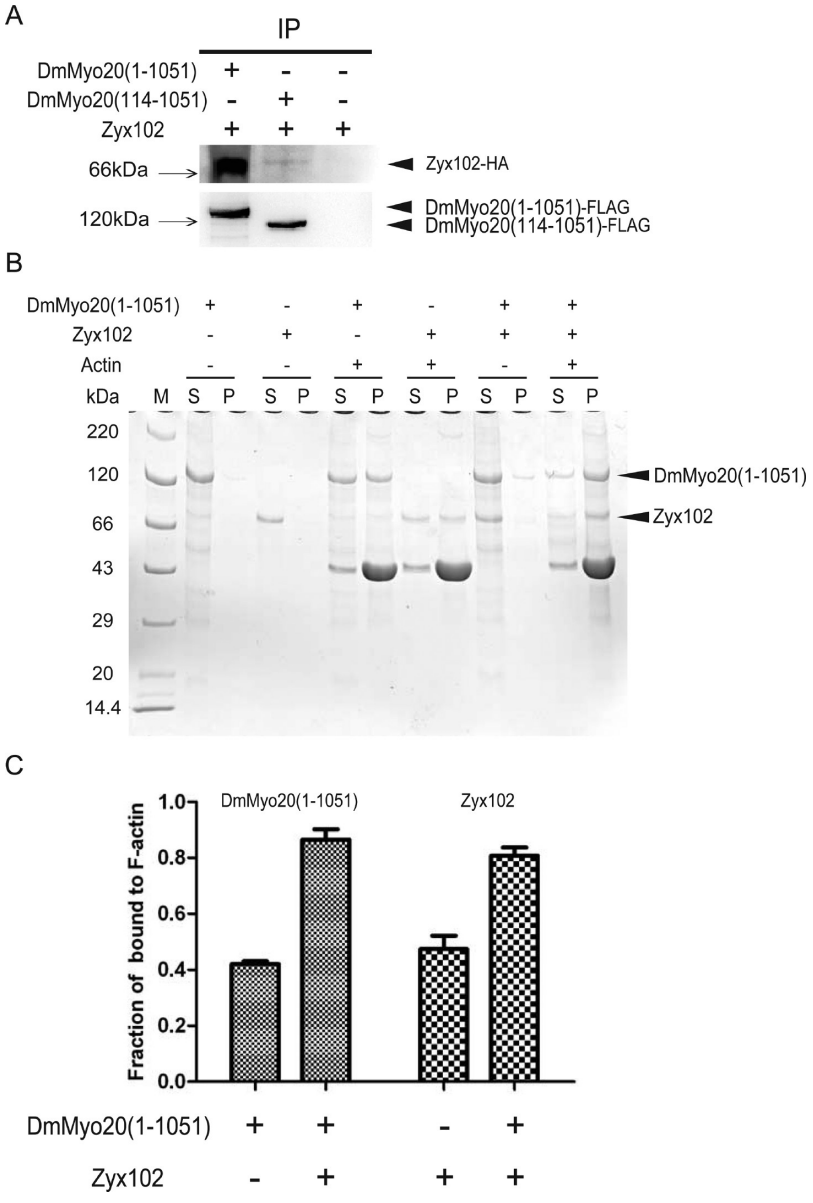

Figure 7. Interaction of DmMyo20, Zyx102, and actin. (A) Co-immunoprecipitation of Zyx102 with DmMyo20(1−1051) and DmMyo20(114−1051). Flag-tagged DmMyo20(1−1051) (0.72 μM) or DmMyo20(114−1051) (0.54 μM) was incubated with HA-tagged Zyx102 (2.8 μM) and then co-immunoprecipitated with anti-Flag agarose. DmMyo20 was detected by anti-Flag antibodies, and Zyx102 was detected by mouse monoclonal anti-HA antibodies. (B) Flag-tagged DmMyo20(1−1051) (0.6 μM) and/or Flag-tagged Zyx102 (0.5 μM) incubated with 10 μM actin and subjected to ultracentrifugation. Equal portions of supernatants and pellets were analyzed by SDS−PAGE and visualized by Coomassie blue staining. The amounts of DmMyo20 and Zyx102 in supernatants and pellets were quantified by densitometry. (C) Data represent the amount of proteins coprecipitated with actin. The ratio of DmMyo20(1−1051) to actin was increased from 42.0 ± 1.7 to 86.6 ± 6.4% (n = 3; mean ± standard deviation) in the presence of Zyx102, and the ratio of Zyx102 to F-actin was increased from 47.4 ± 8.3 to 80.7 ± 5.2% (n = 3; mean ± standard deviation) in the presence of DmMyo20(1−1051).

So far, most characterized myosins bind to F-actin through the motor domain in an ATP-dependent manner: the motor domains bind to F-actin strongly in the absence of ATP and dissociate from F-actin in the presence of ATP. In contrast, we found that the motor domain of DmMyo20 binds to F-actin with a moderate affinity and is insensitive to ATP. In this sense, DmMyo20 is similar to recently characterized motor incompetent myosins, including *Limulus* myosin-3,[34] *Drosophila* myosin-18,[10] and mammalian myosin-18A.[35,36] The affinity of the DmMyo20 motor domain for F-actin (K_d ∼ 40 μM) is comparable to that of the β-isoform of mammalian myosin-18A for F-actin (K_d = 54 μM)[35] but much lower than the affinity of other motor incompetent myosins for F-actin (K_d values of 0.1−10 μM).[10,34−36] The N-terminal extension enhanced the affinity of DmMyo20 for actin 5-fold, suggesting that the N-terminal extension might contain an additional actin-binding site. In this sense, DmMyo20 is very similar to mammalian myosin-18A,[36] which contains an actin-binding site in the N-terminal extension in addition to the actin-binding site in the motor domain. The N-terminal extension of mammalian myosin-18A mediates an ATP-independent binding to F-actin.[36] Unfortunately, we could not detect a direct interaction between the N-terminal extension of DmMyo20 and actin, as

dx.doi.org/10.1021/bi401236c | *Biochemistry* 2014, 53, 350−360

the N-terminal extension constructs of DmMyo20, including DmMyo20(1−113) and DmMyo20(1−280), were insoluble.

Although the affinity of DmMyo20 for F-actin is low *in vitro*, it is possible that other proteins *in vivo* might enhance the affinity. Indeed, we found that Zyx102, a downstream component of DmMyo20 in the Fat signaling pathway, enhanced the interaction between DmMyo20 and F-actin, and conversely, DmMyo20 enhanced the interaction between Zyx102 and F-actin. This finding suggests a novel mechanism of the Fat signaling pathway: the asymmetric localization of the DmMyo20−Zyx102 complex influences the network of actin filaments in the apical region, which in turn influences the increase in *Drosophila* tissue polarity.

In summary, this study demonstrates that DmMyo20 has no ATPase activity but can bind to actin and enhance the interaction between actin and Zyx102. These results suggest that DmMyo20 does not function as a molecular motor but rather as a scaffold protein or an anchoring protein in the signal pathway.

■ ASSOCIATED CONTENT

Supporting Information

Co-immunoprecipitation of Zyx102 and DmMyo20(1−1051) (Figure S1) and actin cosedimentation of DmMyo20(114−1051) and Zyx102 (Figure S2). This material is available free of charge via the Internet at http://pubs.acs.org.

■ AUTHOR INFORMATION

Corresponding Author

*Institute of Zoology, Chinese Academy of Sciences, Beijing 100101, China. Telephone: +86-10-6480-6015. E-mail: lixd@ioz.ac.cn.

Funding

This work was supported by the National Natural Science Foundation of China (31071973), the National Basic Research Program of China (2012CB114102), and the State Key Laboratory of Integrated Management of Pest Insects and Rodents (Chinese IPM1302).

Notes

The authors declare no competing financial interest.

■ ACKNOWLEDGMENTS

We thank Dr. Kenneth D. Irvine (Howard Hughes Medical Institute, Waksman Institute and Department of Molecular Biology and Biochemistry, Rutgers, the State University of New Jersey) for providing plasmid pUAST-d and Huan-Hong Ji and Rong-Na Ma for the preparation of skeletal muscle myosin and smooth muscle myosin HMM, respectively.

■ ABBREVIATIONS

CaM, calmodulin; DmCaM, CaM of *D. melanogaster*; DmMyo20, class XX myosin of *D. melanogaster*; DTT, dithiothreitol; EGTA, ethylene glycol bis(aminoethyl ether)-*N*,*N*,*N*′,*N*′-tetraacetic acid; HMM, heavy meromyosin; SmM, smooth muscle myosin; myosin-5a-S1, truncated myosin-5a containing the motor domain and the first IQ motif; S1, subfragment 1 of smooth muscle myosin.

■ REFERENCES

(1) Odronitz, F., and Kollmar, M. (2007) Drawing the tree of eukaryotic life based on the analysis of 2,269 manually annotated myosins from 328 species. *Genome Biol. 8*, R196.

(2) Mao, Y., Tournier, A. L., Bates, P. A., Gale, J. E., Tapon, N., and Thompson, B. J. (2011) Planar polarization of the atypical myosin Dachs orients cell divisions in *Drosophila*. *Genes Dev. 25*, 131−136.

(3) Breshears, L. M., Wessels, D., Soll, D. R., and Titus, M. A. (2010) An unconventional myosin required for cell polarization and chemotaxis. *Proc. Natl. Acad. Sci. U.S.A. 107*, 6918−6923.

(4) Petzoldt, A. G., Coutelis, J. B., Geminard, C., Speder, P., Suzanne, M., Cerezo, D., and Noselli, S. (2012) DE-Cadherin regulates unconventional Myosin ID and Myosin IC in *Drosophila* left-right asymmetry establishment. *Development 139*, 1874−1884.

(5) Ito, K., Kashiyama, T., Shimada, K., Yamaguchi, A., Awata, J., Hachikubo, Y., Manstein, D. J., and Yamamoto, K. (2003) Recombinant motor domain constructs of *Chara corallina* myosin display fast motility and high ATPase activity. *Biochem. Biophys. Res. Commun. 312*, 958−964.

(6) Nalavadi, V., Nyitrai, M., Bertolini, C., Adamek, N., Geeves, M. A., and Bahler, M. (2005) Kinetic mechanism of myosin IXB and the contributions of two class IX-specific regions. *J. Biol. Chem. 280*, 38957−38968.

(7) O'Connell, C. B., and Mooseker, M. S. (2003) Native Myosin-IXb is a plus-, not a minus-end-directed motor. *Nat. Cell Biol. 5*, 171−172.

(8) Inoue, A., Saito, J., Ikebe, R., and Ikebe, M. (2002) Myosin IXb is a single-headed minus-end-directed processive motor. *Nat. Cell Biol. 4*, 302−306.

(9) Kambara, T., and Ikebe, M. (2006) A unique ATP hydrolysis mechanism of single-headed processive myosin, myosin IX. *J. Biol. Chem. 281*, 4949−4957.

(10) Guzik-Lendrum, S., Nagy, A., Takagi, Y., Houdusse, A., and Sellers, J. R. (2011) *Drosophila melanogaster* myosin-18 represents a highly divergent motor with actin tethering properties. *J. Biol. Chem. 286*, 21755−21766.

(11) Mao, Y., Rauskolb, C., Cho, E., Hu, W. L., Hayter, H., Minihan, G., Katz, F. N., and Irvine, K. D. (2006) Dachs: An unconventional myosin that functions downstream of Fat to regulate growth, affinity and gene expression in *Drosophila*. *Development 133*, 2539−2551.

(12) Foth, B. J., Goedecke, M. C., and Soldati, D. (2006) New insights into myosin evolution and classification. *Proc. Natl. Acad. Sci. U.S.A. 103*, 3681−3686.

(13) Tzolovsky, G., Millo, H., Pathirana, S., Wood, T., and Bownes, M. (2002) Identification and phylogenetic analysis of *Drosophila melanogaster* myosins. *Mol. Biol. Evol. 19*, 1041−1052.

(14) Morgan, T. H., and Bridges, C. B. (1919) The Inheritance of a Fluctuating Character. *J. Gen. Physiol. 1*, 639−643.

(15) Cho, E., and Irvine, K. D. (2004) Action of fat, four-jointed, dachsous and dachs in distal-to-proximal wing signaling. *Development 131*, 4489−4500.

(16) Bosveld, F., Bonnet, I., Guirao, B., Tlili, S., Wang, Z., Petitalot, A., Marchand, R., Bardet, P. L., Marcq, P., Graner, F., and Bellaiche, Y. (2012) Mechanical control of morphogenesis by Fat/Dachsous/Four-jointed planar cell polarity pathway. *Science 336*, 724−727.

(17) Brittle, A., Thomas, C., and Strutt, D. (2012) Planar polarity specification through asymmetric subcellular localization of Fat and Dachsous. *Curr. Biol. 22*, 907−914.

(18) Rogulja, D., Rauskolb, C., and Irvine, K. D. (2008) Morphogen control of wing growth through the Fat signaling pathway. *Dev. Cell 15*, 309−321.

(19) Rauskolb, C., Pan, G., Reddy, B. V., Oh, H., and Irvine, K. D. (2011) Zyxin links fat signaling to the hippo pathway. *PLoS Biol. 9*, e1000624.

(20) Kadrmas, J. L., and Beckerle, M. C. (2004) The LIM domain: From the cytoskeleton to the nucleus. *Nat. Rev. Mol. Cell Biol. 5*, 920−931.

(21) Coudrier, E., and Almeida, C. G. (2011) Myosin 1 controls membrane shape by coupling F-actin to membrane. *Bioarchitecture 1*, 230−235.

(22) Spudich, J. A., and Watt, S. (1971) The regulation of rabbit skeletal muscle contraction. I. Biochemical studies of the interaction of

the tropomyosin-troponin complex with actin and the proteolytic fragments of myosin. *J. Biol. Chem. 246*, 4866−4871.
(23) Li, X. D., Jung, H. S., Mabuchi, K., Craig, R., and Ikebe, M. (2006) The globular tail domain of myosin Va functions as an inhibitor of the myosin Va motor. *J. Biol. Chem. 281*, 21789−21798.
(24) Li, X. D., Mabuchi, K., Ikebe, R., and Ikebe, M. (2004) Ca^{2+}-induced activation of ATPase activity of myosin Va is accompanied with a large conformational change. *Biochem. Biophys. Res. Commun. 315*, 538−545.
(25) Lu, Z., Shen, M., Cao, Y., Zhang, H. M., Yao, L. L., and Li, X. D. (2012) Calmodulin bound to the first IQ motif is responsible for calcium-dependent regulation of myosin 5a. *J. Biol. Chem. 287*, 16530−16540.
(26) Li, X., Ikebe, R., and Ikebe, M. (2005) Activation of myosin Va function by melanophilin, a specific docking partner of myosin Va. *J. Biol. Chem. 280*, 17815−17822.
(27) Ma, R. N., Mabuchi, K., Li, J., Lu, Z., Wang, C. L., and Li, X. D. (2013) Cooperation between the Two Heads of Smooth Muscle Myosin Is Essential for Full Activation of the Motor Function by Phosphorylation. *Biochemistry 52*, 6240−6248.
(28) Pollard, T. D. (1982) Myosin purification and characterization. *Methods Cell Biol. 24*, 333−371.
(29) Zhu, T., Beckingham, K., and Ikebe, M. (1998) High affinity Ca^{2+} binding sites of calmodulin are critical for the regulation of myosin Iβ motor function. *J. Biol. Chem. 273*, 20481−20486.
(30) Li, X. D., Rhodes, T. E., Ikebe, R., Kambara, T., White, H. D., and Ikebe, M. (1998) Effects of mutations in the γ-phosphate binding site of myosin on its motor function. *J. Biol. Chem. 273*, 27404−27411.
(31) Kodama, T., Fukui, K., and Kometani, K. (1986) The initial phosphate burst in ATP hydrolysis by myosin and subfragment-1 as studied by a modified malachite green method for determination of inorganic phosphate. *J. Biochem. 99*, 1465−1472.
(32) Ostapchuk, P., and Hearing, P. (2008) Adenovirus IVa2 protein binds ATP. *J. Virol. 82*, 10290−10294.
(33) Forgacs, E., Cartwright, S., Kovács, M., Sakamoto, T., Sellers, J. R., Corrie, J. E. T., Webb, M. R., and White, H. D. (2006) Kinetic mechanism of myosinV-S1 using a new fluorescent ATP analogue. *Biochemistry 45*, 13035−13045.
(34) Kempler, K., Toth, J., Yamashita, R., Mapel, G., Robinson, K., Cardasis, H., Stevens, S., Sellers, J. R., and Battelle, B. A. (2007) Loop 2 of limulus myosin III is phosphorylated by protein kinase A and autophosphorylation. *Biochemistry 46*, 4280−4293.
(35) Guzik-Lendrum, S., Heissler, S. M., Billington, N., Takagi, Y., Yang, Y., Knight, P. J., Homsher, E., and Sellers, J. R. (2013) Mammalian Myosin-18A, a Highly Divergent Myosin. *J. Biol. Chem. 288*, 9532−9548.
(36) Taft, M. H., Behrmann, E., Munske-Weidemann, L. C., Thiel, C., Raunser, S., and Manstein, D. J. (2013) Functional Characterization of Human Myosin-18A and Its Interaction with F-actin and GOLPH3. *J. Biol. Chem. 288*, 30029−30041.
(37) Heeley, D. H., Belknap, B., and White, H. D. (2006) Maximal activation of skeletal muscle thin filaments requires both rigor myosin S1 and calcium. *J. Biol. Chem. 281*, 668−676.
(38) Maruta, H., and Korn, E. D. (1981) Direct photoaffinity labeling by nucleotides of the apparent catalytic site on the heavy chains of smooth muscle and Acanthamoeba myosins. *J. Biol. Chem. 256*, 499−502.
(39) Staley, B. K., and Irvine, K. D. (2012) Hippo signaling in *Drosophila*: Recent advances and insights. *Dev. Dyn. 241*, 3−15.
(40) Crawford, A. W., Michelsen, J. W., and Beckerle, M. C. (1992) An interaction between zyxin and α-actinin. *J. Cell Biol. 116*, 1381−1393.
(41) Smith, C. A., and Rayment, I. (1996) X-ray structure of the magnesium(II)·ADP·vanadate complex of the *Dictyostelium discoideum* myosin motor domain to 1.9 Å resolution. *Biochemistry 35*, 5404−5417.
(42) Shimada, T., Sasaki, N., Ohkura, R., and Sutoh, K. (1997) Alanine scanning mutagenesis of the switch I region in the ATPase site of *Dictyostelium discoideum* myosin II. *Biochemistry 36*, 14037−14043.
(43) Fisher, A. J., Smith, C. A., Thoden, J. B., Smith, R., Sutoh, K., Holden, H. M., and Rayment, I. (1995) X-ray structures of the myosin motor domain of *Dictyostelium discoideum* complexed with MgADP·BeF_x and MgADP·AlF_4^-. *Biochemistry 34*, 8960−8972.
(44) Sasaki, N., Shimada, T., and Sutoh, K. (1998) Mutational analysis of the switch II loop of *Dictyostelium* myosin II. *J. Biol. Chem. 273*, 20334−20340.